

Center for Advanced Materials

CAM

RECEIVED
LAWRENCE
BERKELEY LABORATORY

MAY 24 1988

Submitted to Journal of Electronic Materials
LIBRARY AND DOCUMENTS SECTION

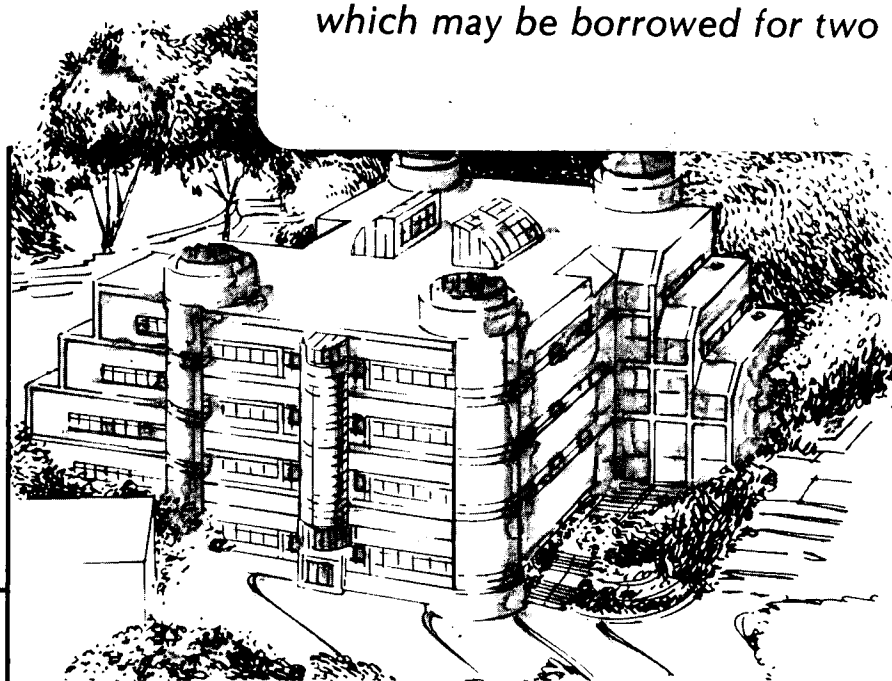
Stress Relaxation in 60Sn-40Pb Solder Joints

D. Tribula, D. Grivas, J.W. Morris, Jr.

February 1988

TWO-WEEK LOAN COPY

*This is a Library Circulating Copy
which may be borrowed for two weeks.*



Materials and Chemical Sciences Division
Lawrence Berkeley Laboratory • University of California
ONE CYCLOTRON ROAD, BERKELEY, CA 94720 • (415) 486-4755

LBL-24815
e.2

DISCLAIMER

This document was prepared as an account of work sponsored by the United States Government. While this document is believed to contain correct information, neither the United States Government nor any agency thereof, nor the Regents of the University of California, nor any of their employees, makes any warranty, express or implied, or assumes any legal responsibility for the accuracy, completeness, or usefulness of any information, apparatus, product, or process disclosed, or represents that its use would not infringe privately owned rights. Reference herein to any specific commercial product, process, or service by its trade name, trademark, manufacturer, or otherwise, does not necessarily constitute or imply its endorsement, recommendation, or favoring by the United States Government or any agency thereof, or the Regents of the University of California. The views and opinions of authors expressed herein do not necessarily state or reflect those of the United States Government or any agency thereof or the Regents of the University of California.

STRESS RELAXATION IN 60Sn-40Pb SOLDER JOINTS

D. Tribula, D. Grivas, J. W. Morris, Jr.

Center for Advanced Materials
Materials and Chemical Sciences Division
Lawrence Berkeley Laboratory
University of California

and

Department of Materials Science and Mineral Engineering
University of California, Berkeley
Berkeley, California 94720

February 1988

This work is jointly supported by the Director, Office of Energy Research,
Office of Basic Energy Science, Materials Sciences Division of the
U. S. Department of Energy under Control No. DE-AC03-76SF00098

STRESS RELAXATION IN 60Sn-40Pb SOLDER JOINTS

D. Tribula, D. Grivas, J.W. Morris, Jr.

Center for Advanced Materials

Lawrence Berkeley Laboratory

Department of Materials Science and Mineral Engineering

University of California, Berkeley, CA 94720

The stress relaxation behaviour of 60Sn-40Pb solder in a joint configuration was investigated over a range of temperatures and two starting stresses. Unlike the bulk 60Sn-40Pb alloy, the deformation behaviour of the joint could not be described by a power law dependence between strain rate and stress. In fact, the joint relaxation was found to depend on the starting stress level; higher starting stress levels relaxed much faster than lower starting stresses. Microstructural analysis of the deformed joint revealed extensive grain boundary sliding and inter Sn-Sn grain cracking.

INTRODUCTION

A Sn-Pb solder joint in an electronic package typically joins materials of different thermal expansion characteristics, for example a ceramic chip carrier to a polymeric circuit board. With each temperature excursion, the unequal thermal expansion of the constraining interfaces shears the solder joint. In service, repeated thermal cycling due to environmental changes and power cycling, fatigues the solder joint, ultimately causing its failure. Thermal fatigue experiments on representative solder joints are among the first steps to understanding and eventually improving the material's fatigue resistance. However, since the solder is typically used at very high homologous temperature, creep and stress relaxation phenomena are probably significant. Therefore, prior to the design of a fatigue experiment, knowledge of the time response of a stressed solder joint is needed.

Such information is, in fact, available for certain bulk Sn-Pb microstructures: the high-temperature steady-state deformation of certain Sn-Pb alloys is represented by

$$d\gamma/dt = A\tau^n d^m e^{-\Delta H/kT} \quad (1)$$

where γ is the steady-state shear strain rate, τ is the shear stress and d is an effective grain size^{1,2,3}. Integration of this equation and substitution of the appropriate constants yields the desired stress/time behaviour of the alloy. However, the relevance of this power law to the stress relaxation behaviour of a very small volume of as-cast Sn-Pb constrained between two interfaces, i.e. a solder joint, is unknown.

This work examined the stress relaxation of a 60Sn-40Pb solder joint. The specimens, which contained a small volume of Sn-Pb joining two Cu plates, were geometrically suitable for testing on a standard load frame. Stress/time data were collected for several specimens as a function of temperature and initial stress. The validity of a power law representation of the relaxation data was tested. SEM microstructural observations of these joints are also reported.

EXPERIMENTAL

To manufacture specimens, three plates of oxygen free, 99.99% pure Cu were polished, etched, and fluxed. The joint assembly was immersed, under vacuum, into a molten solder bath, 60wt% Sn-40wt% Pb both of 99.99% purity. After cooling and removal of excess solder, the assembly was machined and sectioned to yield the specimen shown in figure 1.

Each specimen block yields 8 to 10 0.065" (1.7mm) thick specimens. The composition and processing history are thus constant within each specimen set.

Stress relaxation tests were performed starting from an initial stress attained on a screw-driven load frame at a cross-head speed of 0.0005"/min (0.0127mm/min). Data were collected at various temperatures starting from two different initial stresses. A "temperature equivalent" stress is defined as a fixed fraction of the joint's shear strength at that temperature. The following temperature baths were used: -55°C, liquid nitrogen cooled ethanol; 0°C, ice water; 25°C, air; 55°C, 100°C, heated silicon oil.

RESULTS

Relaxation Data

Representative stress-strain curves at 0°C and 55°C appear in figure 2. The open and closed circles each correspond to temperature equivalent stresses, henceforth referred to as the high stress and low stress specimens, respectively.

The stress decay data for all temperatures and both starting stresses are plotted in figure 3. The solid lines represent relaxation from the lower equivalent stress (open circles, figure 2); the dashed lines show decay from the higher starting stress. For the more highly stressed specimens stress relaxation is very rapid: at 0°C the stress relaxed to two thirds its initial value in 10 minutes and complete relaxation was attained after 200 minutes; at 55°C the stress relaxed to two thirds its initial value after only two minutes and complete relaxation was attained after 80 minutes. The relaxation of the less stressed specimens is much slower: at 0°C the stress relaxed to two thirds its initial value after 150 minutes and complete relaxation was not attained even after several days; at 55°C the stress relaxed to two third its initial value in 60 minutes and, again, complete relaxation was not attained. In all cases, the relaxation rate of the higher stressed specimens is faster than relaxation from the lower initial stress level. Furthermore, complete relaxation was attained only for the initially higher stressed specimens.

To determine the applicability of a power law, such as equation (1), the data were plotted as $\log(d\tau/dt)$ vs $\log(\tau)$, figure 4. Due to the high compliance of the machine used in these experiments $d\gamma/dt \propto d\tau/dt$, and the data can be plotted as $d\tau/dt$ vs τ without loss of generality of (1). Linearity indicates a power law dependence between strain rate and stress. Inspection of figure 4 shows that no single empirical relationship is able to describe all the data. However, within a single stress level the data appear qualitatively similar. All the high stress data are linear, and the three high temperature data sets are parallel. In

contrast, none of the lower stress data are linear on this type of plot; however, the curve shapes representing the three different specimens are similar.

Microstructure

The initial joint microstructure appears in figure 5. Regions of lamellar and globular two-phase microstructure, primary Pb-rich phase, and interfacial and bulk intermetallic phases are visible. As identified in previous work², the interfacial phases are Cu_3Sn and Cu_6Sn_5 ; the latter also occurs in the bulk of the joint as long, hexagonal, hollow rods.

In figures 6a and 6b the joint surfaces are shown as they appear immediately after deformation. No surface preparation has taken place, yet the various phases are easily distinguishable. Cracking, figure 6a, as well as extensive grain boundary movement, figure 6b, has occurred. Both displacements occur primarily in the Sn/Sn grain boundaries and, to a lesser extent, at the Sn/Pb interface. A polished joint surface of a typical high stress specimen appears in figure 7. The intergranular cracking of the Sn-rich phase persists into the bulk of the joint. Grain boundary sliding was also quite evident in the low stress specimens; however, the extent of Sn/Sn grain cracking was severely diminished in these joints.

DISCUSSION

Compliance with an equation similar to (1), as displayed by bulk Sn-Pb alloys, is readily identified as a linear relationship between $\log(\text{strain rate})$ vs. $\log(\text{stress})$ plot. The slope of this line, m in equation (1), is characteristic of the rate controlling deformation mechanism operative in this strain rate range^{1,2,3}. Inspection of figure 4 reveals that a universal application of equation (1) to the current data set is not possible.

In addition, a dependence on the initial stress level is seen. Specimens relaxing from a high initial stress relax much faster and to a lower final stress than do equivalent, initially less-stressed specimens. The microstructural damage, as revealed by SEM, introduced on loading seems the most probable reason for this anomalous behaviour. Wild⁴ reports similar relaxation behaviour, however, without accompanying microstructural data.

Beyond this dependence on initial stress, certain qualitative similarities in relaxation behaviour within a given stress level are apparent. As a group, the high stress data share common features: the stress decay rate is linear in the given plot, and several data sets are parallel. Linearity indicates activity of a single relief mechanism over this range of strain rates; similar slopes, exhibited by the high temperature data, imply stress relief via similar

deformation mechanisms over this temperature range. In contrast, the nonlinear behaviour of the low stress data set may be interpreted as a transition state in which no single (or unique combination of) mechanism(s) dominates. The similarity between the curves for the three temperatures indicates a similar transition decay.

The SEM observations reveal extensive grain boundary sliding and intergranular cracking. Furthermore, these displacements are localized to the Sn/Sn grain boundaries and Sn/Pb interphase boundaries. These observations are in qualitative agreement with other work on similar microstructures. Grain boundary sliding measurements performed on a worked and recrystallized Sn-Pb eutectic⁵ reveal different grain boundary sliding susceptibilities for the various interfaces: the largest measured sliding offsets are for the Sn/Sn grain boundaries, smaller offsets are reported for the Sn/Pb interphase boundaries and little or no sliding of Pb/Pb grain boundaries.

The shear strain experienced by a solder joint joining a polymeric chip carrier to a ceramic printed circuit board on a -55°C to 125°C temperature change is ~20%⁶. The experimental joint strains in this work range from 20 to >100%, and the data indicate that only the high stresses, i.e. those responsible for the largest strains, relax appreciably within a short time. The experimental joint strained 20% at room temperature retains 90% of the initial stress for well over 24 hours. The stress relaxation effects in fatigue where similar strain ranges, cycle times, and temperatures exist are thus expected to be small.

CONCLUSIONS

For the stresses studied, 60Sn-40Pb solder joint stress relaxation is dependent on the starting stress level. Higher initial stresses relax more quickly and more completely than do lower initial stresses. Small scale intergranular cracking within the joint, as revealed by SEM, may account for the initial stress level dependence. Furthermore, it is not possible to represent all the relaxation data in terms of a power law similar to that of the bulk 60Sn-40Pb. However, the microstructural deformation of the 60Sn-40Pb solder joint appears qualitatively similar to that of the bulk material.

ACKNOWLEDGMENTS

This work is supported by the Director, Office of Energy Research, Office of Basic Energy Science, Materials Science Division of the U.S. Department of Energy under contract #DE-AC-3-76SF00098.

FIGURE CAPTIONS

Figure 1. Experimental solder joint configuration.

Figure 2. Stress/strain data of solder joint at 0°C and 55°C. The open and closed circles each represent a fixed fraction of the joint's shear strength (a "temperature equivalent stress").

Figure 3. Stress relaxation data as a function of starting stress and temperature. The solid and dashed lines correspond to relaxation from low initial stress and high initial stress, respectively. Each solid and dashed data pair corresponds to a single temperature, as labelled.

Figure 4. Relaxation data plotted as $\log (d\tau/dt)$ vs. $\log (\tau)$. The circles represent all specimens relaxing from the higher initial stress, the triangles relaxation from the lower initial stress.

Figure 5. SEM image of the initial joint microstructure.

Figure 6. SEM micrograph of joint microstructure immediately after deformation. Small cracks between Sn-Sn grains are visible (a), and evidence of Sn-Sn grain boundary sliding is apparent in (b).

Figure 7. A polished solder joint. The inter Sn-Sn grain cracking persists into the bulk of the joint material.

REFERENCES

1. B.P. Kashyap, G.S. Murty, Mat. Sci. Eng. **50** p. 205 (1981).
2. D. Grivas, Ph.D. Thesis, University of California at Berkeley, Berkeley, CA (1979).
3. G.S. Murty, J. Mat. Sci. **8** p. 611 (1973).
4. D. Frear, D. Grivas, J.W. Morris, Jr., J. Electronic Materials, **16** p.181 (1987)
5. R.N. Wild, IBM report #747000481, October 1975.
6. P. Shariat, B. Ramsevak, B. Vastava, T.G. Langdon, Acta Met. **30** p.285 (1982).
7. D. Frear, Ph.D. Thesis, University of California at Berkeley, Berkeley, CA (1987).

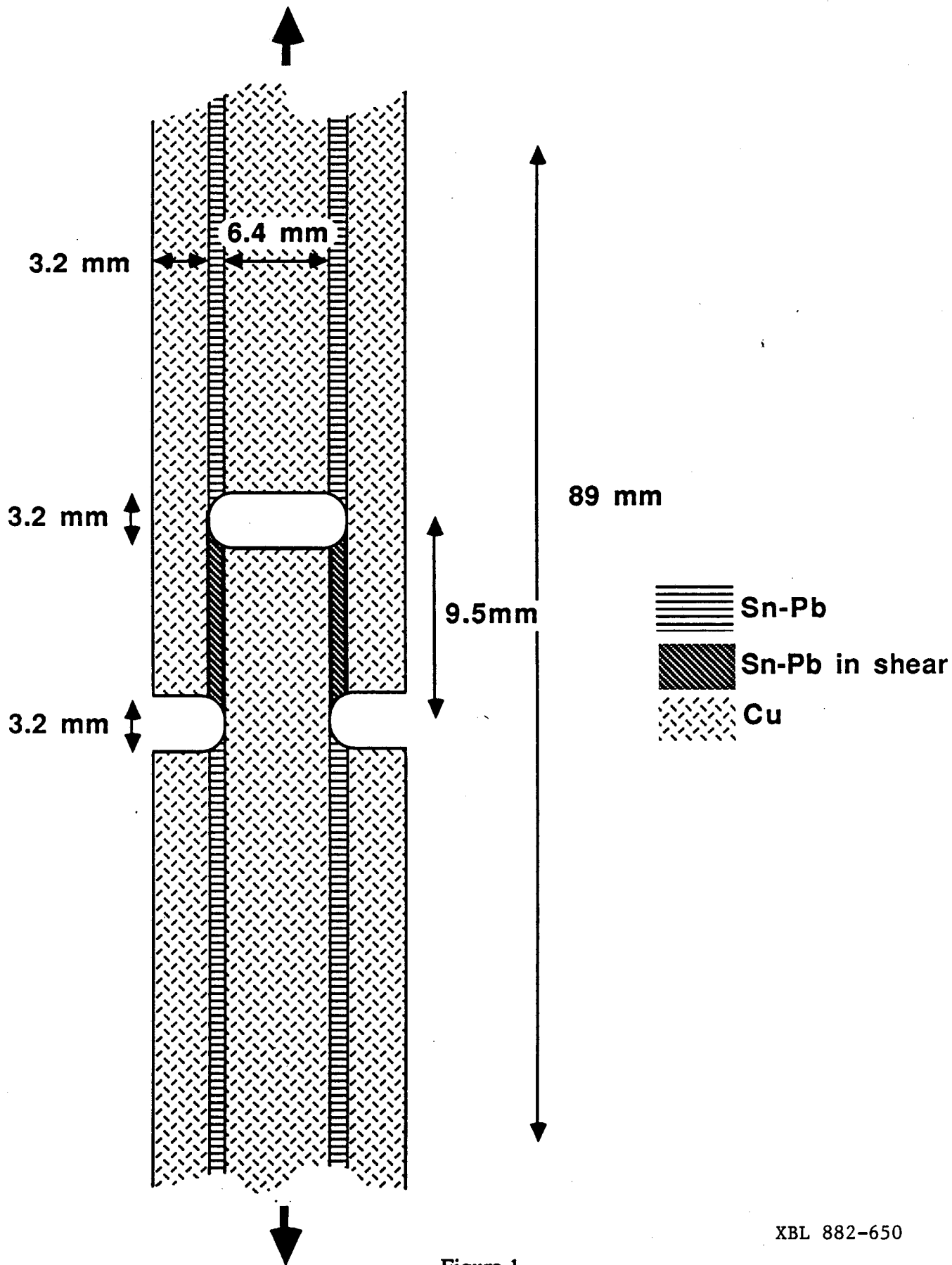
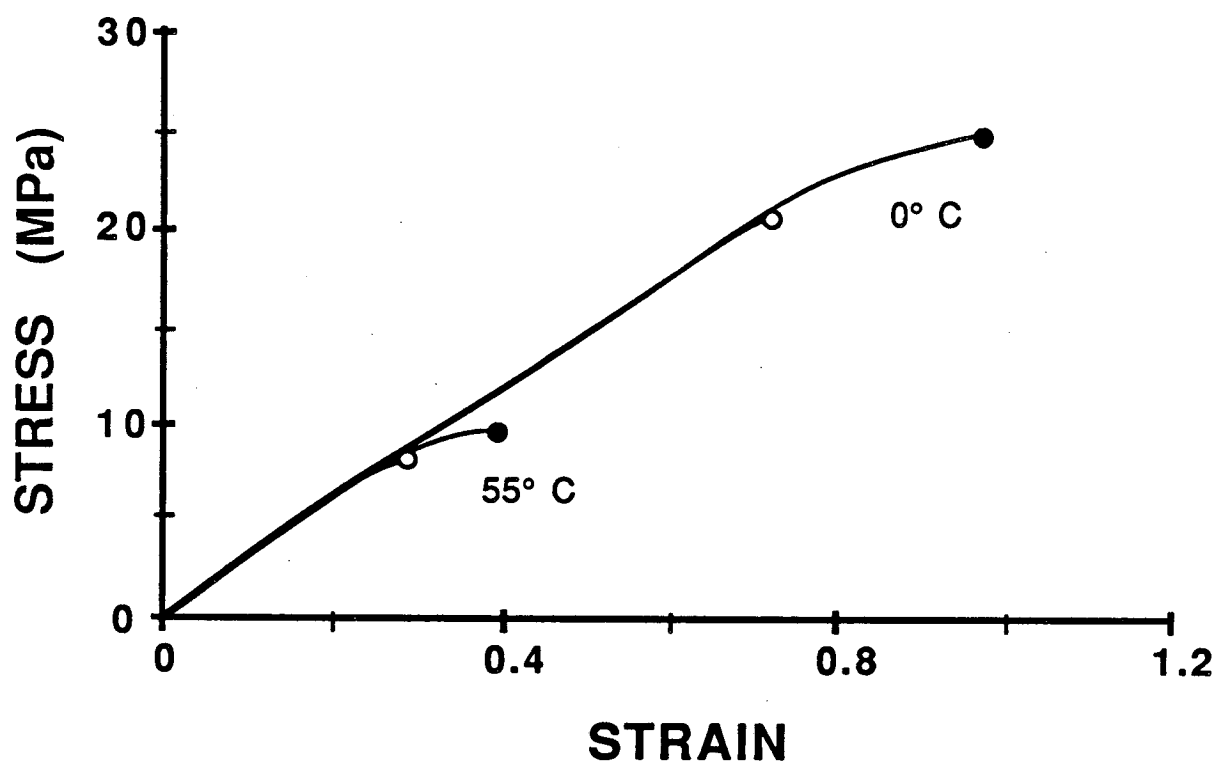


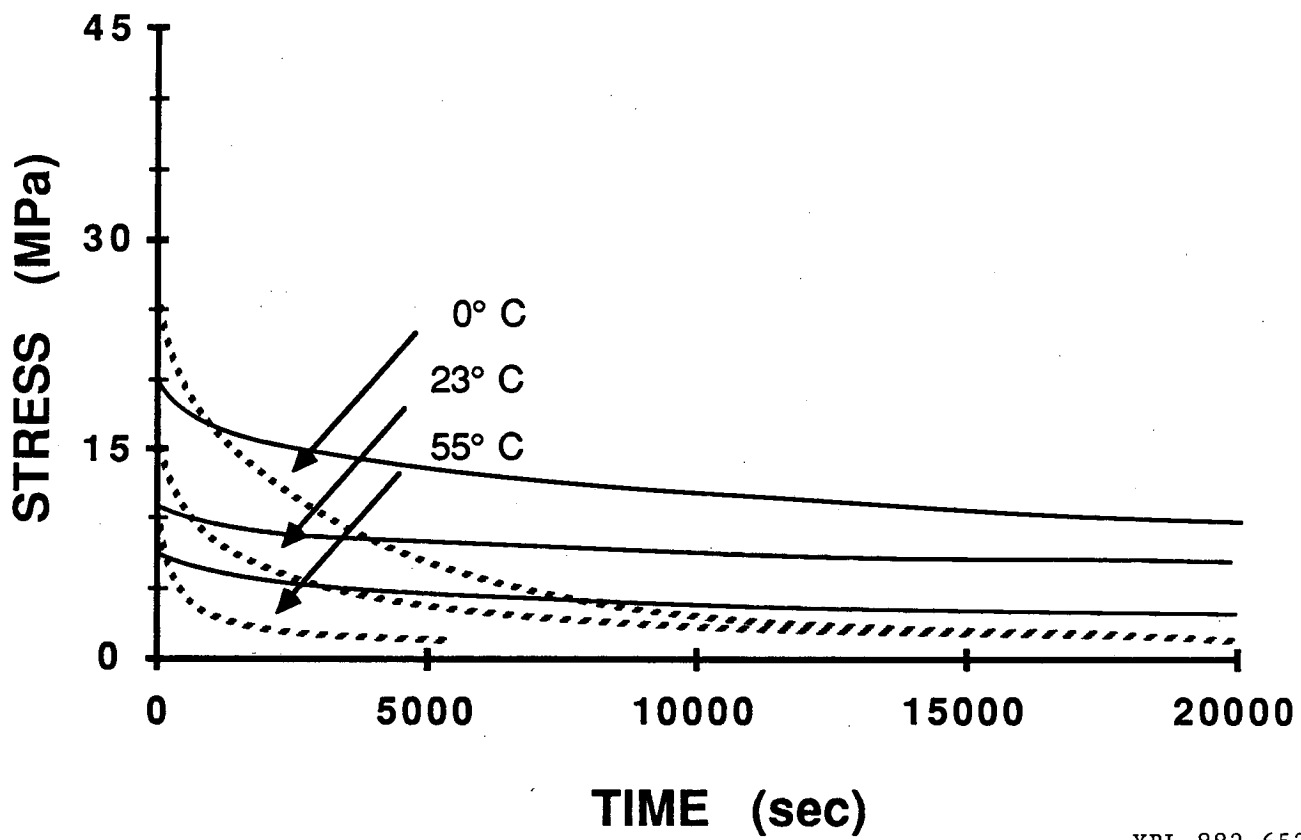
Figure 1.

XBL 882-650



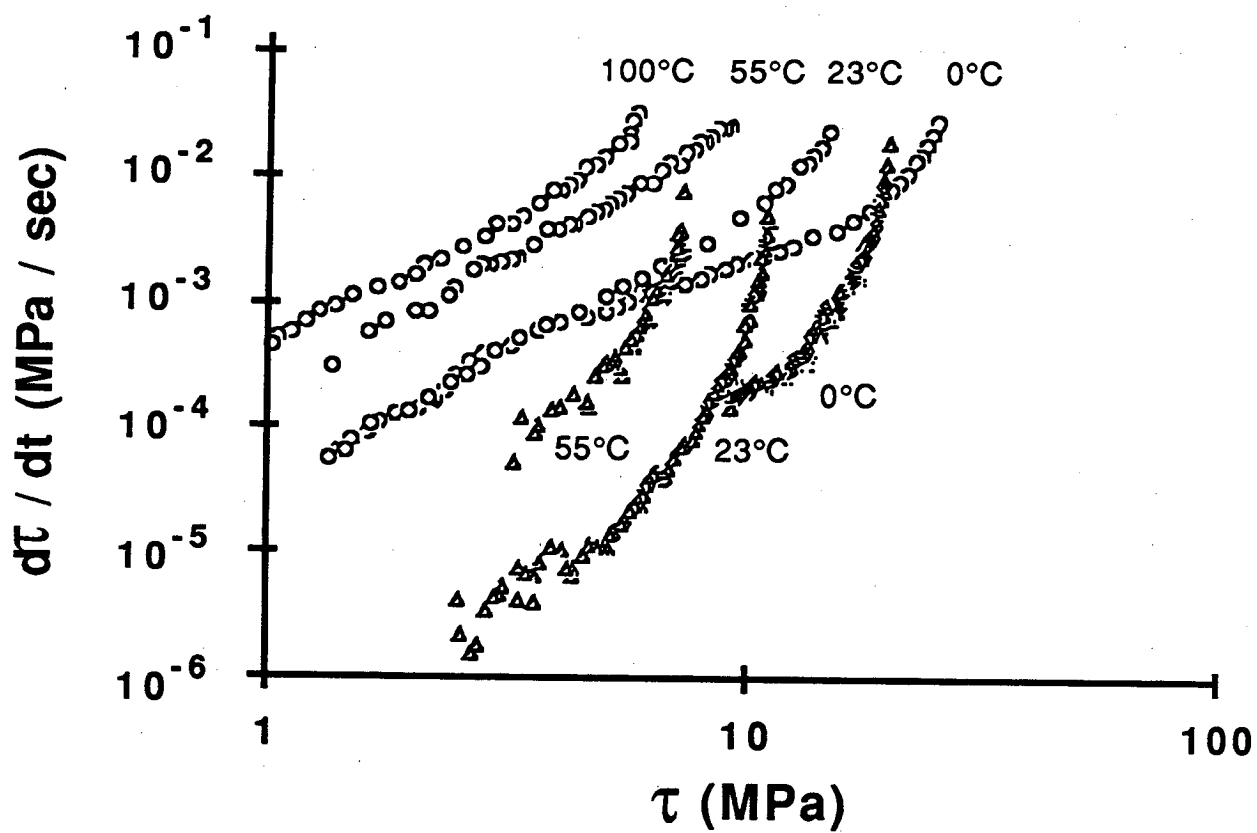
XBL 882-651

Figure 2.



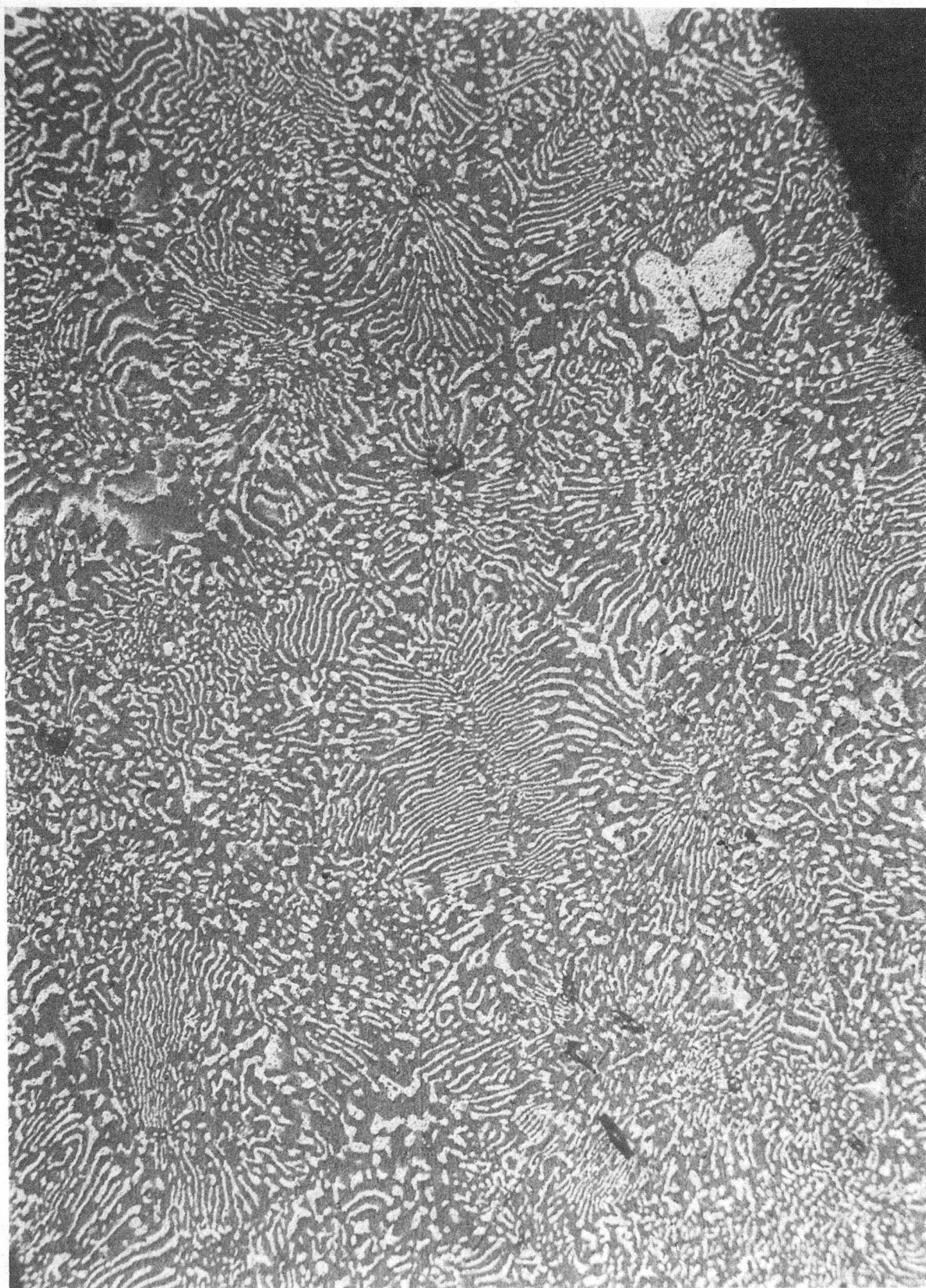
XBL 882-652

Figure 3.



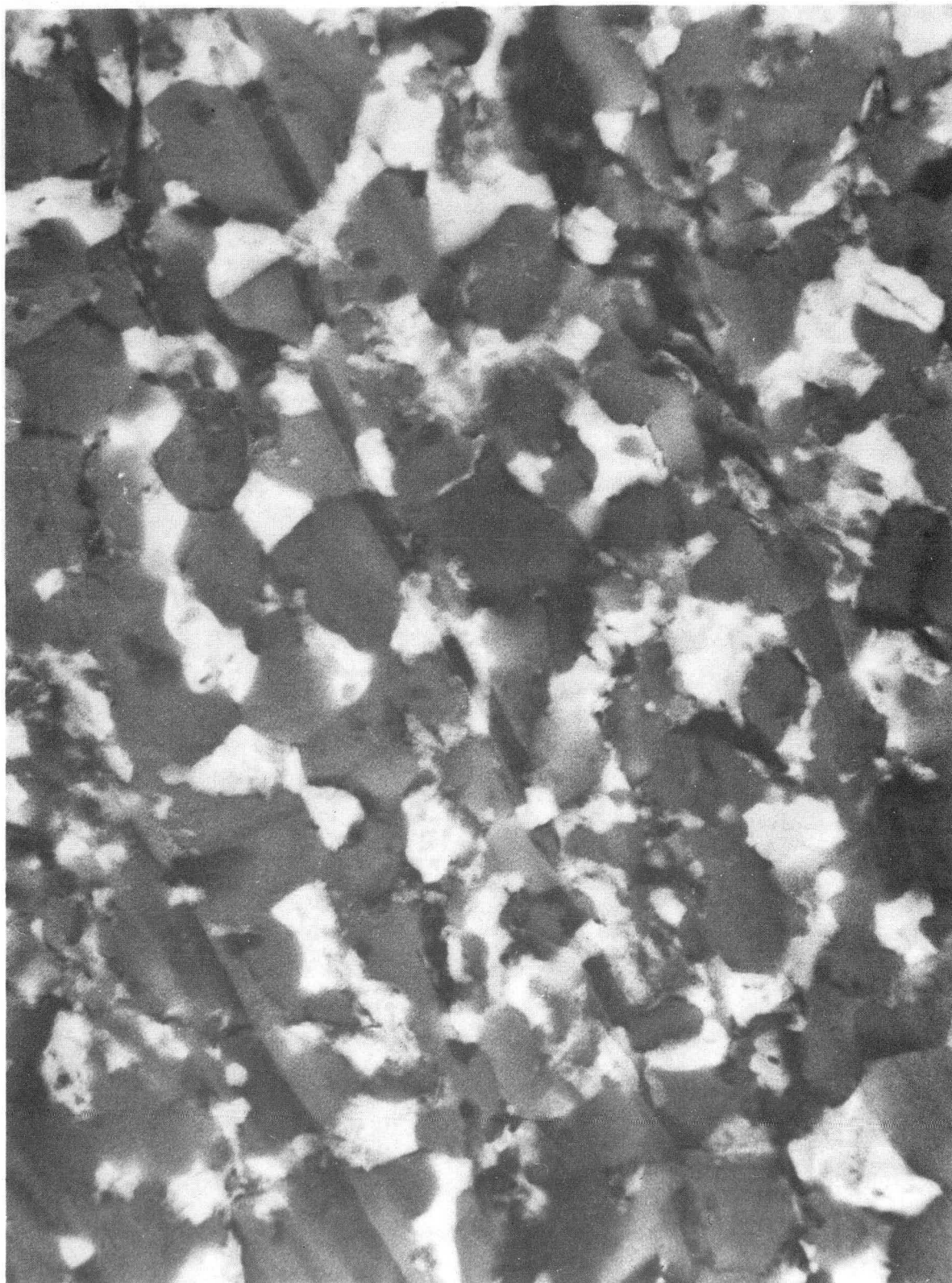
XBL 882-653

Figure 4.



XBE 872--1197

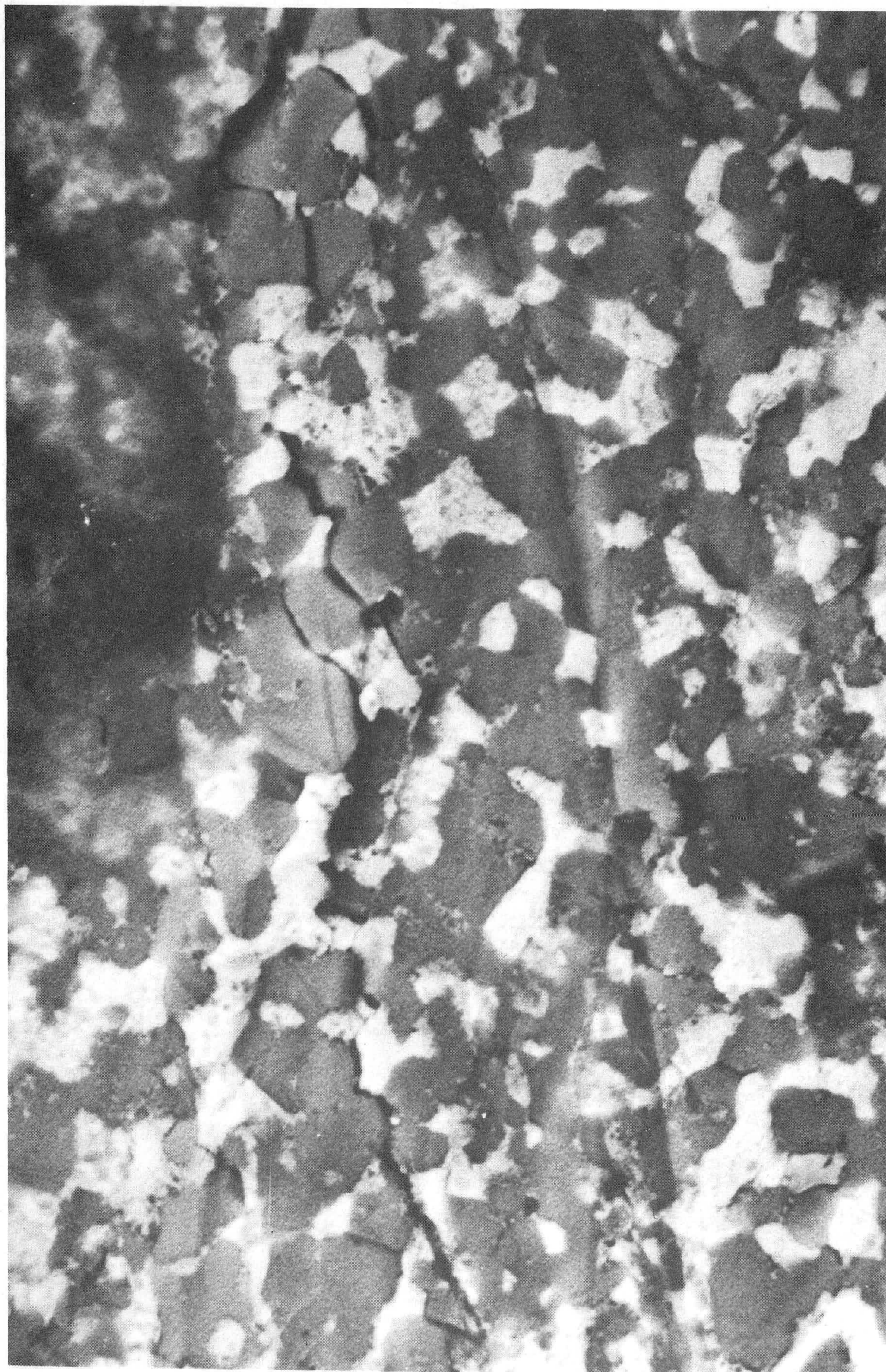
Figure 5



5.0 μm

Figure 6a

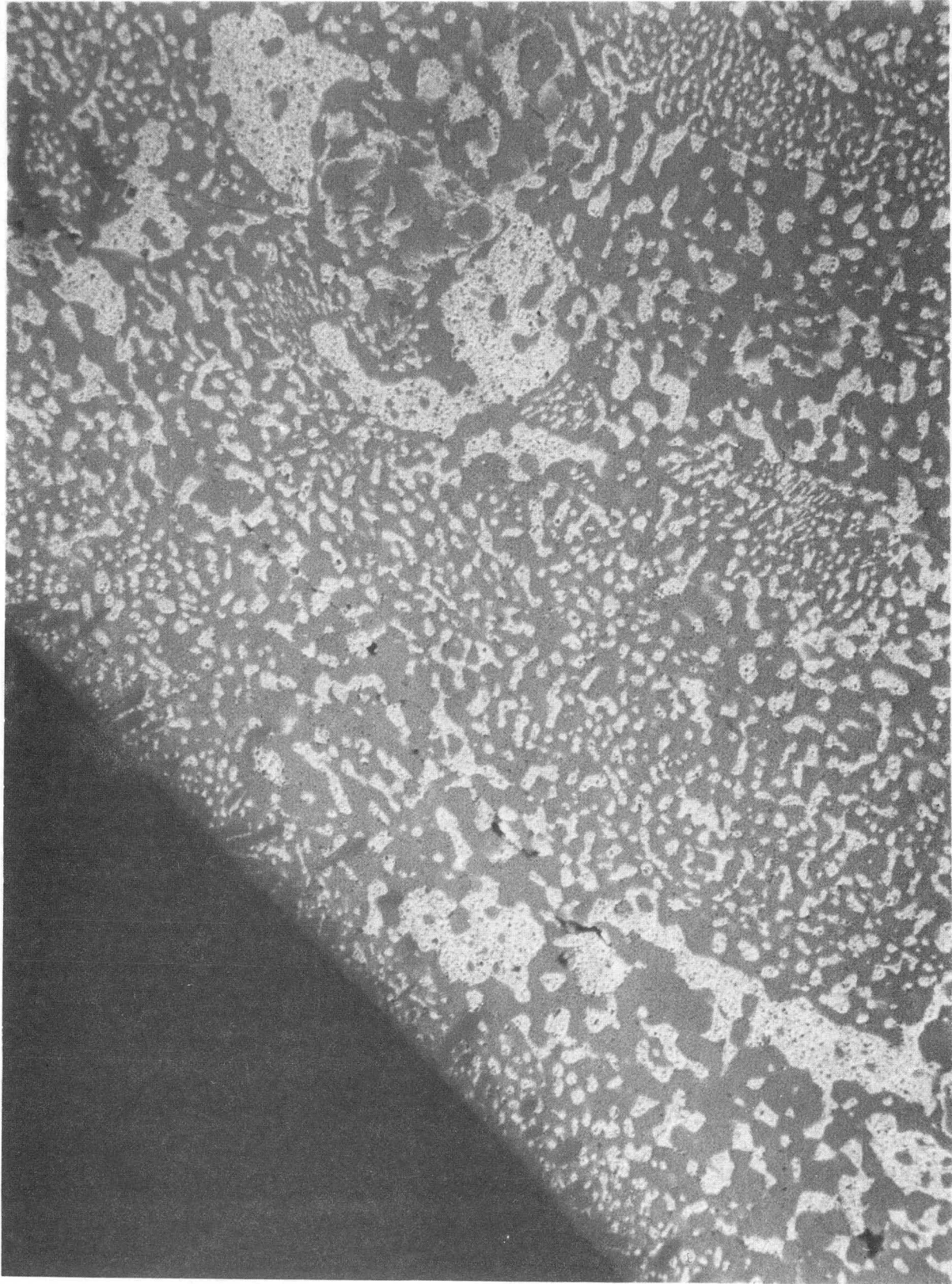
XBB872--1199



5.0 μm

Figure 6b

XBB871-654



XBB 872-1198

Figure 7

LAWRENCE BERKELEY LABORATORY
TECHNICAL INFORMATION DEPARTMENT
UNIVERSITY OF CALIFORNIA
BERKELEY, CALIFORNIA 94720